Bibliographie

[1] J. A. SHERCLIFF, *A Textbook of Magnetohydrodynamics* (Pergamon Press, Oxford 1965).
[2] G. W. SUTTON and A. S. SHERMAN, *Engineering Magnetohydrodynamics* (McGraw-Hill, New York 1965).
[3] J. L. NEURINGER, J. Fluid Mech. *7*, 287 (1960).
[4] S. E. DREYFUS, *Dynamic Programming and the Calculus of Variations* (Academic Press, New York 1965).
[5] R. E. BELLMAN and S. E. DREYFUS, *Applied Dynamic Programming* (Princeton Univ. Press, Princeton 1962).

Résumé

On traite le problème des conditions de maximum de conversion d'énergie dans les générateurs magnétohydrodynamique pour les écoulements incompressibles et compressibles, et pour les cas ou les électrodes sont répartis soit en sections finies soit en sections continues. Les conditions d'optimalité sont trouvées pour les cas finis par le principe de Bellman, et pour le cas de repartition infinie des électrodes par l'équation fondamentale de la programmation dynamique.

(Received: October 7, 1970)

Nonlinear Analysis of Flow Pulses and Shock Waves in Arteries

Part II: Parametric Study Related to Clinical Problems[1])

By Max Anliker, Robert L. Rockwell[2]), Dept. of Aeronautics and Astronautics, Stanford University, Stanford, California, and Eric Ogden, Environmental Biology Division, Ames Research Center, NASA, Moffett Field, California, USA

V. Variations in Diameter and Wave Speed

The effects of a general reduction of the mean diameter of the aorta by 20% (which amounts to a decrease in cross-sectional area by 36%) have been evaluated using the method of characteristics and the equations derived in Part I. All other parameter values are the same as in the Standard Case and the results are given in Figures 23 and 24. A decrease in the cross-sectional area apparently causes higher flow velocities and pulse pressures. The velocity is higher because the same amount of blood must flow through the smaller aorta (the stroke volume remains 30 cm^3). The pulse pressure is increased as a consequence of lowering the distensibility of the artery by reducing the cross-sectional area. With ϱ and $c(p, z)$ unchanged, a 36% decrease in S means a decrease in the distensibility $(\partial S/\partial p)_z$ by the same percentage according to equation (10). If the dicrotic wave is a manifestation of reflections emanating from the distal segment of the arterial conduit where we have a small diameter (and thus a

[1]) For Part I see Z. ang. Math. Phys. *22*, 217 (1971).
[2]) Now, Naval Weapons Center, China Lake, California.

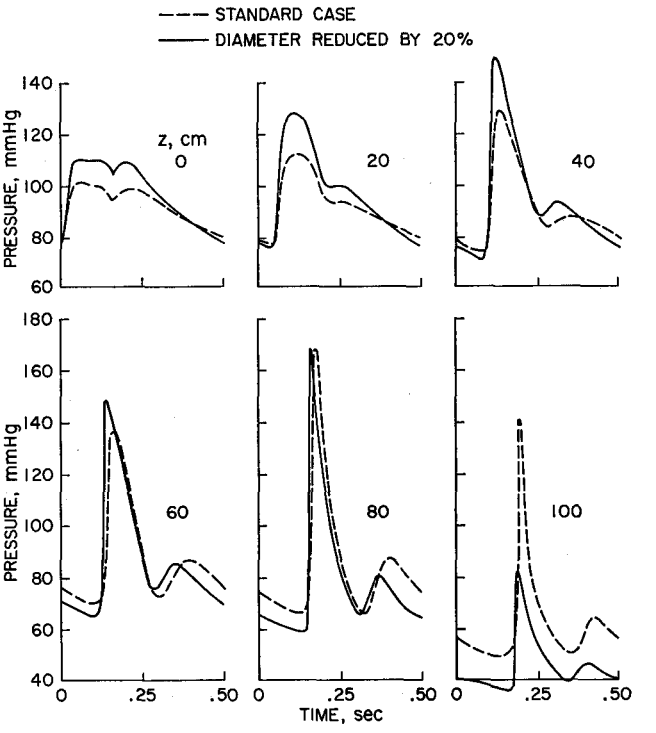

Figure 23
Pressure-time profiles at various distances from the heart for reduced arterial diameters, with other cardiovascular parameters unchanged from the Standard Case.

relatively stiff tube), the overall reduction in diameter should lead to a dicrotic wave which is more distinct at closer distances from the heart than in the Standard Case. Figures 23 and 24 seem to confirm this. Also, as z increases, the diastolic pressure assumes lower values than in the Standard Case, which appears to be due to the larger outflow from the proximal aorta due to the higher pressures during systole. The higher pressures also lead to higher average wave speeds which in turn cause the pressure peaks to occur earlier in time.

It is known that the wave speed in arteries increases with age [35] and possibly also as a result of atherosclerosis. We have therefore examined the effects of a general increase in wave speed by 40% which, according to the Moens-Korteweg equation, is equivalent to a doubling of the elastic modulus of the vessel wall. Since any increase in wave speed amounts to a reduction of the distensibility, we expect the pressure and flow pulses to exhibit similar changes, as in the case of a general reduction in the diameter. Indeed, the results shown in Figures 25 and 26 confirm this. We note again a higher systolic pressure and a steeper wave front. The pressure peaks and valleys occur much earlier due to the increase in wave speed. However, the flow pulse is not as strongly affected by a 40% increase in wave speed which amounts to a lowering of the distensibility by 96%, as it is by a decrease in the distensibility by 36% through a reduction in the cross-sectional area without a change in wave speed. The higher wave speed also appears to induce what could be interpreted as the onset of a second dicrotic wave at the larger distances from the heart.

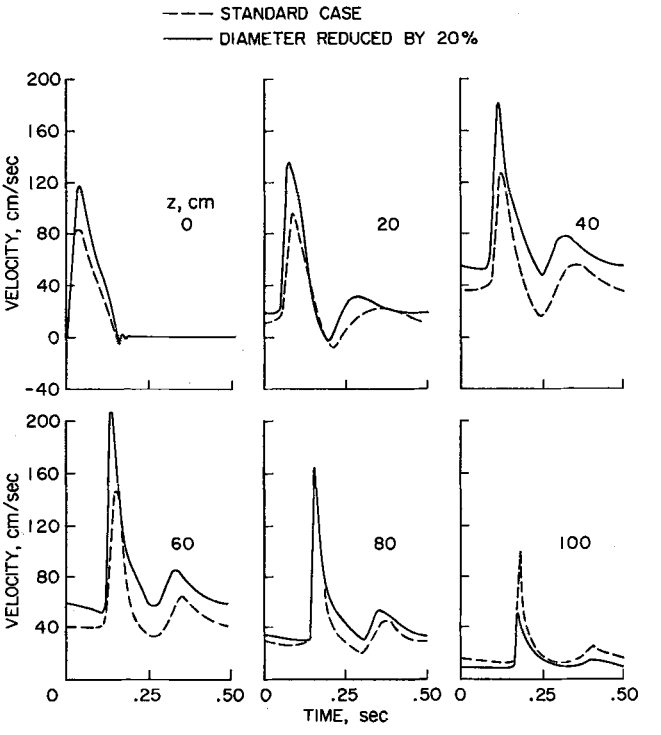

Figure 24
Velocity-time profiles at various distances from the heart for reduced arterial diameters, with other cardiovascular parameters unchanged from the Standard Case.

VI. Changes in Pulse Rate and Stroke Volume

Figures 27 and 28 display the effects of changing the heart rate from the standard value of 120 to 180 and 60 beats per minute. The systolic interval, i.e., the ejection time, was left unchanged and the stroke volume was also held constant. Therefore the cardiac output was changed by factors of 3/2 and 1/2, respectively. Since physiologic responses will cause changes in the outflow pattern when the cardiac output is altered to this degree, the outflow constant was changed by the same factor in each case. Thus the pulse rate of 180 per minute is taken to simulate exercise, and 60 per minute to simulate rest. We recognize that these variations are only gross approximations. For example, in exercise certain organs receive more blood and others less which means that scaling the outflow distribution by changing γ is somewhat artificial.

For the lower pulse rate of 60 beats per minute, the pulse pressure is generally larger than in the Standard Case because we have also reduced γ for this case and therefore increased the resistance to outflow while the ejection phase of the cardiac cycle is the same as the Standard Case. We note that a short interval of negative flow persists well past $z = 40$ cm. Also, we find additional 'dicrotic waves'. Actually, such additional waves during diastole were observed experimentally on anesthetized dogs [27]. It is of interest that the first extra wave appears to coincide in time with the next primary wave of the Standard Case. A similar statement can be made about the second extra wave, which has a relatively small amplitude, and the dicrotic wave

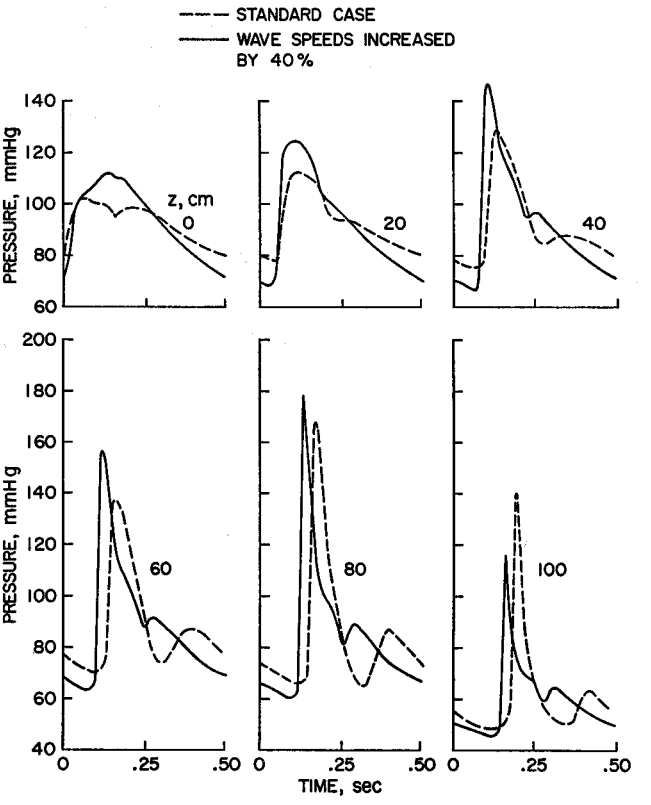

Figure 25
Pressure-time profiles for wave speeds 40% higher than with the Standard Case, but with all other cardiovascular parameters unaltered. As expected, the pressure peaks and valleys develop earlier in time for the higher wave speeds.

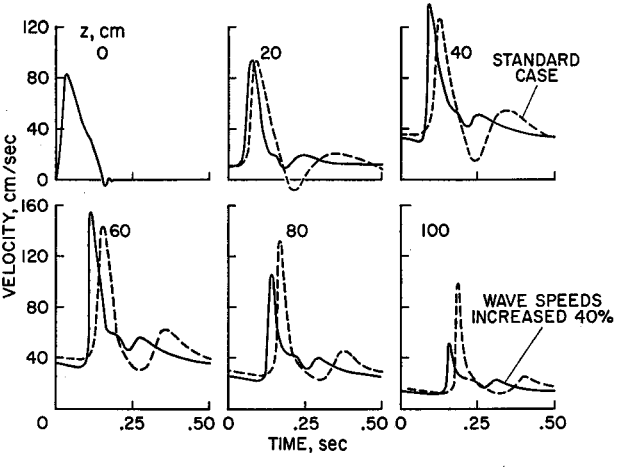

Figure 26
Velocity-time profiles for wave speeds 40% higher than with the Standard Case, but with all other cardiovascular parameters unaltered. With higher wave speeds or stiffer vessels the phenomenon of flow reversal is increasingly restricted to shorter distances from the heart.

of the Standard Case. This suggests that some of the prominent features of the natural pulse are directly related to reflection phenomena.

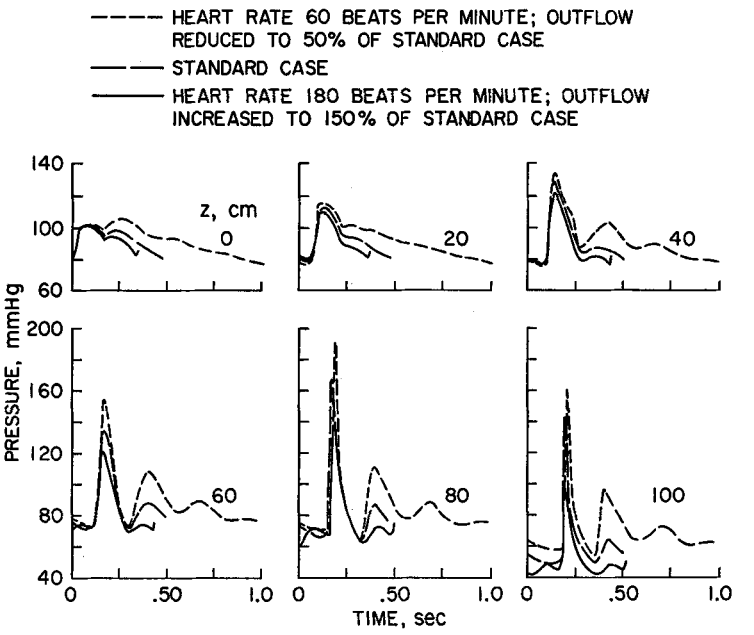

Figure 27
Pressure-time profiles showing the effect of heart rates different from that of the Standard Case (H.R. = 120 beats per minute). The outflow constant γ was adjusted as indicated in order to maintain essentially the same diastolic pressure at the heart.

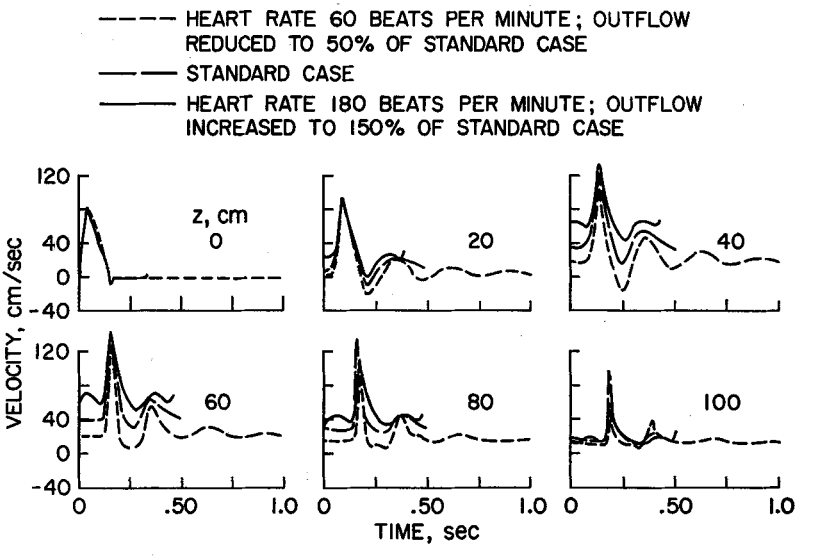

Figure 28
Velocity-time profiles for different heart rates corresponding to the pressure curves of Figure 27.

The increase in pulse rate from 120 to 180 beats per minute generally leads to opposite effects relative to the Standard Case than does a reduction in heart rate from 120 to 60. The pulse pressure is diminished since we have lowered the outflow resistance. Also, the short interval of negative flow is no longer present at $z = 20$ cm.

The result of altering the stroke volume was studied for both larger (50 cm^3) and smaller (20 cm^3) values than in the Standard Case (30 cm^3). To allow for an examination

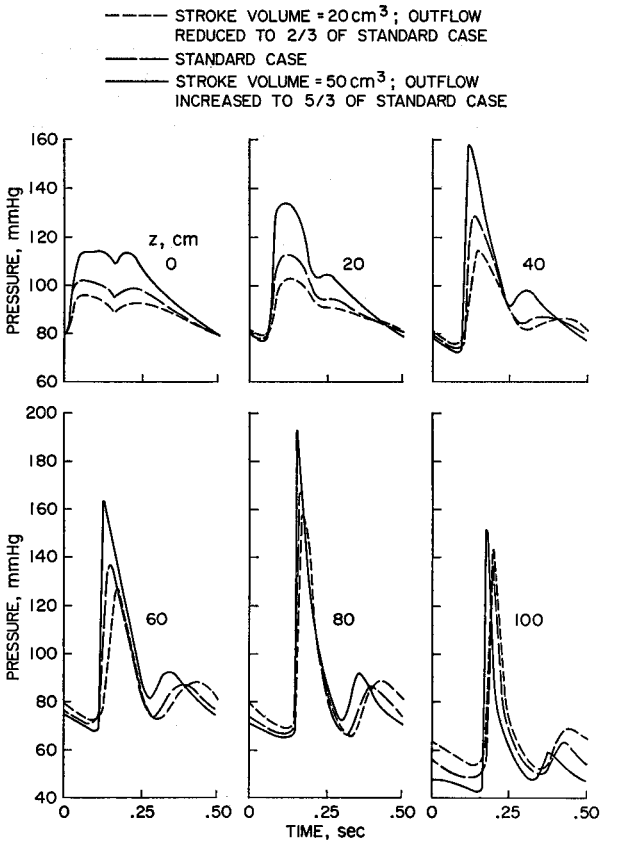

Figure 29
Effect of stroke volume on the pressure pattern. The cardiac ejection rates used were obtained by scaling the ejection rates given in Figure 7. The outflow constant γ was changed by the same factor, but all other parameter values are those of the Standard Case. As expected, the pulse pressure varies in a direct manner with the stroke volume. Also, with increasing pressure the peaks and valleys of the pressure pulse are advanced in time.

of the effects of stroke volume at near normal diastolic pressure levels, the outflow was adjusted by a corresponding factor. All other cardiovascular parameters were left unchanged. Therefore, an increase in the stroke volume should produce an increase in the pressure and flow pulses while conversely a decrease in stroke volume should diminish them. Accordingly, we expect a more pronounced steepening of the wave front at the higher stroke volume and a more gradual one when we reduce it. We note that the results plotted in Figures 29 and 30 confirm these predictions. The flow pulse patterns given in Figure 30 also indicate that for the small stroke volume we have reversal even at relatively large distances from the heart.

VII. Generalized Vasoconstriction and Vasodilatation and Effects of a Change in Outflow Distribution

Generalized vasoconstriction and vasodilatation relative to the Standard Case can be simulated in the model by altering the resistance to outflow through the outflow constant γ. This is only a partial simulation because the diameter of the artery of interest was kept constant. If we select a smaller value for γ, we produce a vasoconstriction which in turn should cause an increase in the mean pressure and in the

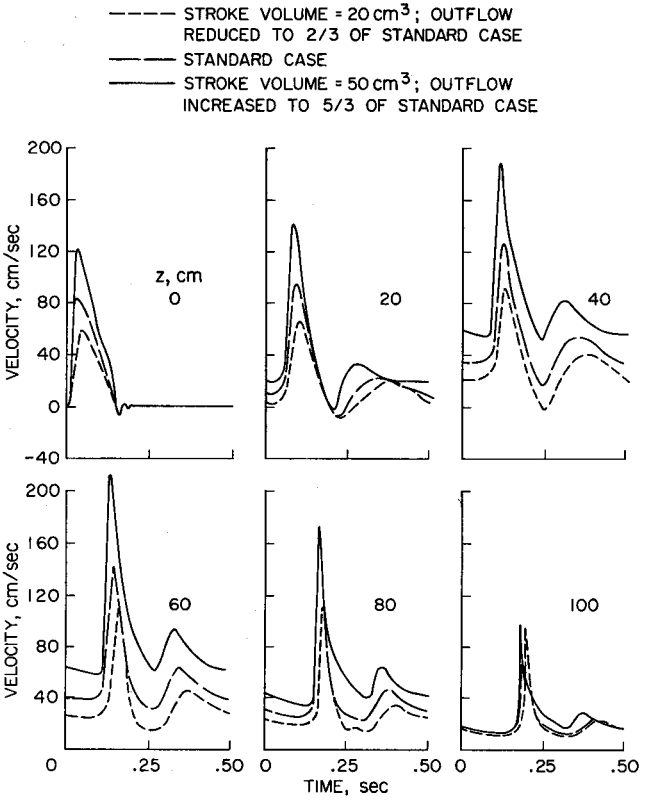

Figure 30
Velocity patterns corresponding to different values of the stroke volume and pressure patterns shown in Figure 29.

pulse pressure because less blood is being removed from the artery while the stroke volume is the same as before. The pressure rise should lead to larger wave speeds and therefore pulses which travel somewhat faster. For vasodilatation, the effects must be antithetic.

These expectations are corroborated by Figures 31 and 32 where the outflow constant γ was changed by $\pm$ 15%. The Standard Case is also plotted for comparison purposes and naturally falls between the two sets of curves illustrating the effects of vasodilatation and vasoconstriction. From Figure 32 we conclude that the pressure rise induced by increasing the outflow resistance has apparently caused a sufficiently large distension of the proximal aorta to lower the peak and mean flow velocities.

As stated in Section II, the model for outflow pattern ψ is not entirely satisfactory. In order to assess the effects of the variation of ψ with distance along the artery, we have modified the outflow function of the Standard Case to simulate what might occur as a result of reducing the outflow into the abdomen as illustrated in Figure 33. Since we are leaving the outflow constant and the cardiac output unchanged, the pressure must increase. This is corroborated by the results shown in Figure 34. A higher pressure leads in turn to an increase in the outflow rates and a larger distension of the vessel which together account for the reduction in the flow pulse evident in Figure 35. The results given in Figures 34 and 35 show that any marked

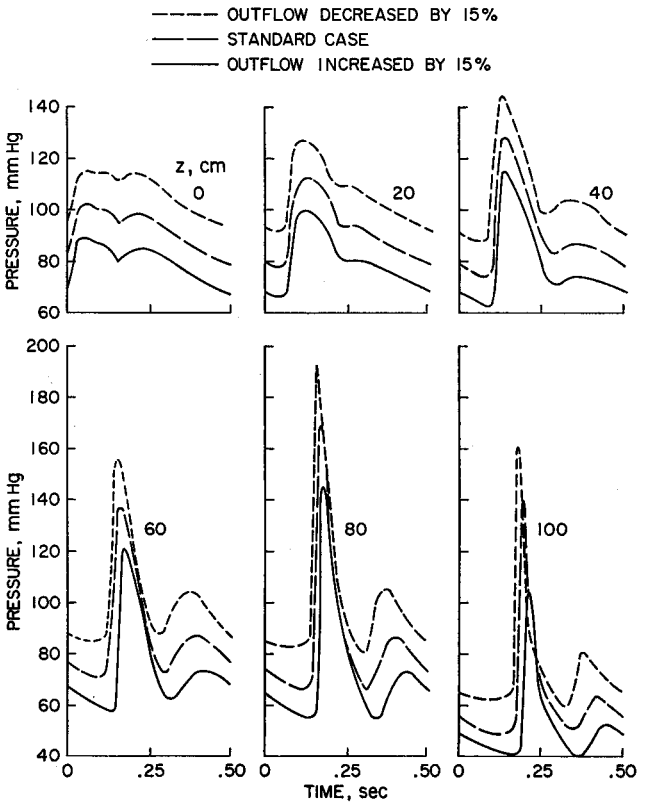

Figure 31
Effects of generalized vasoconstriction and vasodilatation on the pressure pulse produced by changing the outflow constant γ by $\pm$ 15% in the Standard Case.

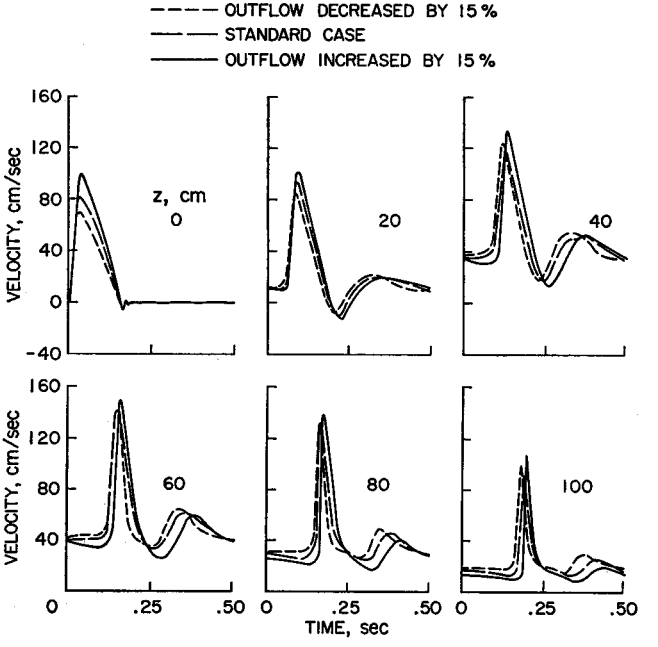

Figure 32
Velocity patterns for generalized vasoconstriction and vasodilatation produced by changing the outflow constant γ by $\pm$ 15% in the Standard Case.

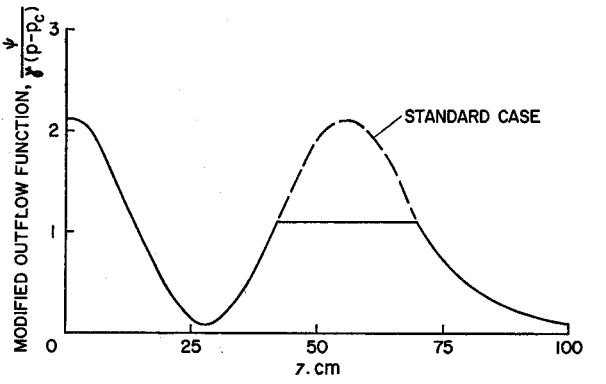

Figure 33
Outflow distribution function (solid curve) used to simulate reduction of blood flow into the abdomen by approximately 1/3.

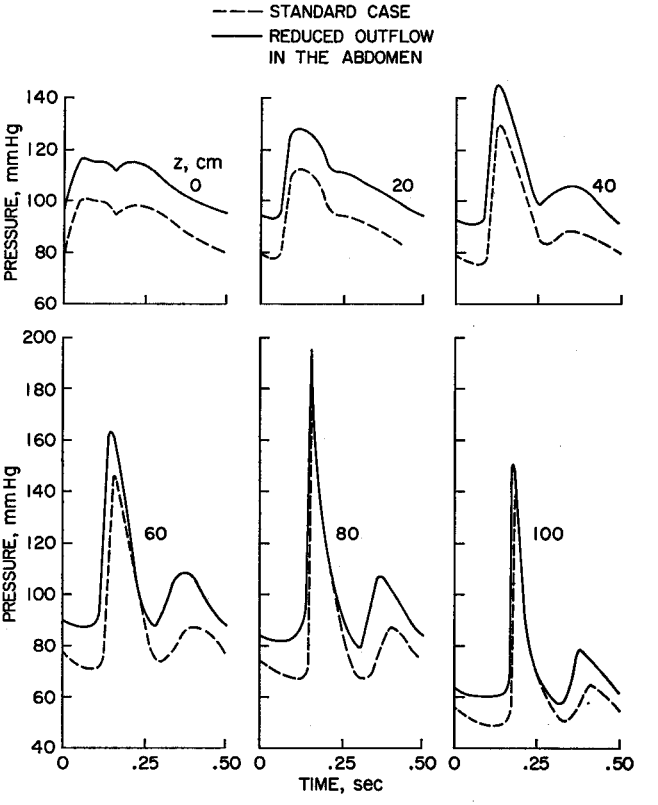

Figure 34
Pressure profiles computed using the outflow function of Figure 33, all other parameter values and functions remaining unchanged.

change in outflow distribution, with all other cardiovascular parameters left unaltered, should cause clearly noticeable deviations from the Standard Case.

VIII. Cardiac Arrest and a Quiescent State as Initial Conditions

Cardiac arrest was simulated by setting the cardiac ejection rate to zero after steady state was reached for the Standard Case. The results are given in Figure 36

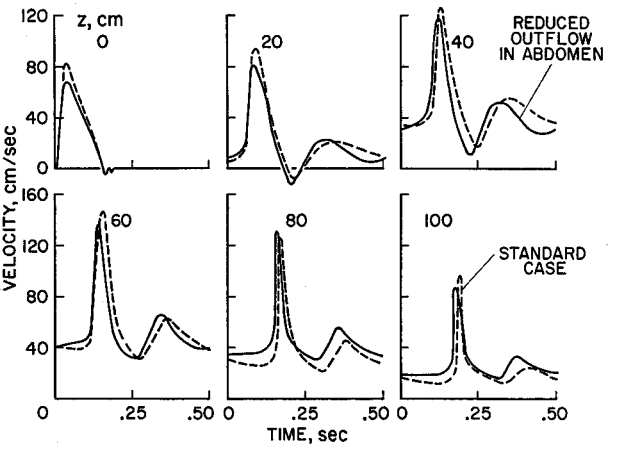

Figure 35
Velocity profiles corresponding to the modified outflow distribution shown in Figure 33 and to the pressure pattern given in Figure 34.

and show the presence of small fluctuations in pressure and velocity after the ejection has ceased. It appears that these fluctuations, including the dicrotic wave, are manifestations of multiple reflections of the primary waves. But the dicrotic wave or any other wave cannot be interpreted as a simple reflection at a discrete site because all pressure and flow peaks or valleys tend to appear later in time as the pulse travels down the artery. Retrograde waves should appear earlier in the distal and later in the proximal regions. No distinct retrograde waves can be discerned in Figure 36. The reflection mechanisms which seem to be responsible for the development of the dicrotic wave have yet to be identified in a quantitative manner.

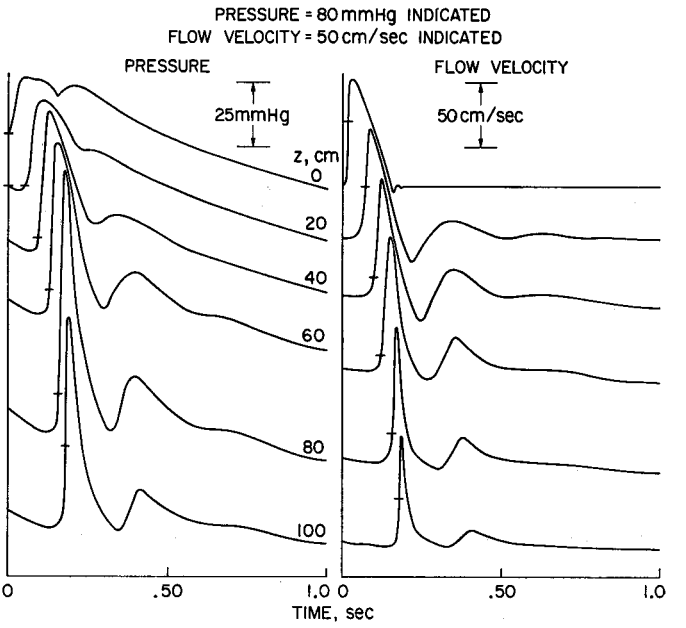

Figure 36
Effect of cardiac arrest on the pressure and flow patterns of the Standard Case. On the left we have indicated the pressure corresponding to 80 mm Hg at the beginning of each profile, while on the right the horizontal marks define the points at which the mean flow has reached a velocity of 50 cm/sec.

If we are interested in steady state pressure and flow profiles, the choice of initial conditions is not crucial. However, in order to minimize the computations, we have regularly prescribed the initial conditions in terms of guesses for the ultimate end-diastolic pressures and flow. It was generally found that, for all practical purposes, the actual steady state condition was reached after two heart beats when the end-diastolic pressure at the heart was estimated to within a few mm Hg and when the end-diastolic velocity pattern of the Standard Case was used as the initial velocity distribution.

In a few situations, the nature of the initial conditions may be pertinent, for example, in determining the response of the cardiovascular system to renewed cardiac activity following a state of cardiac arrest. We now consider such a situation and assume that the period of cardiac arrest is sufficiently long to produce in our model a quiescent state characterized by zero velocity and a pressure of 25 mm Hg ($= p_c$ so that there is no outflow) everywhere in the artery. With such a quiescent state as initial conditions and for cardiovascular parameters corresponding to the Standard

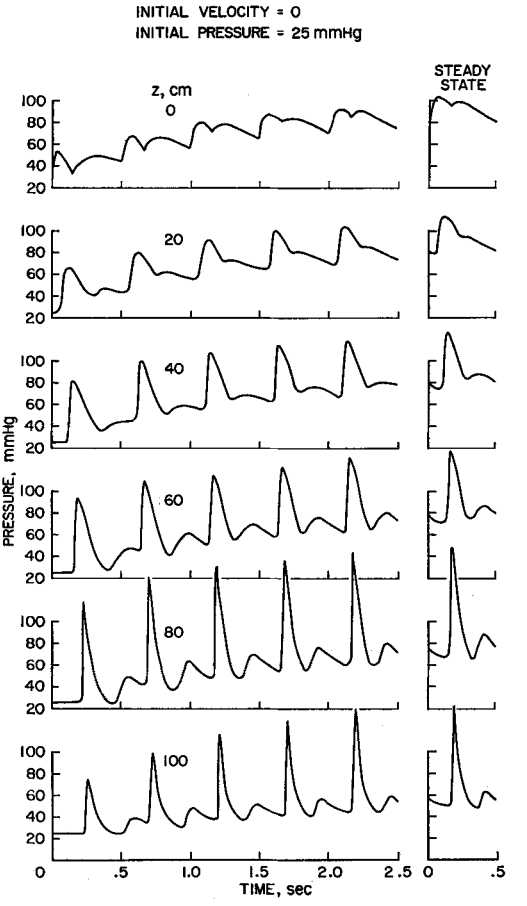

Figure 37
Pressure profiles for the Standard Case caused by a normal cardiac ejection pattern after a period of cardiac arrest sufficiently long to produce a quiescent state.

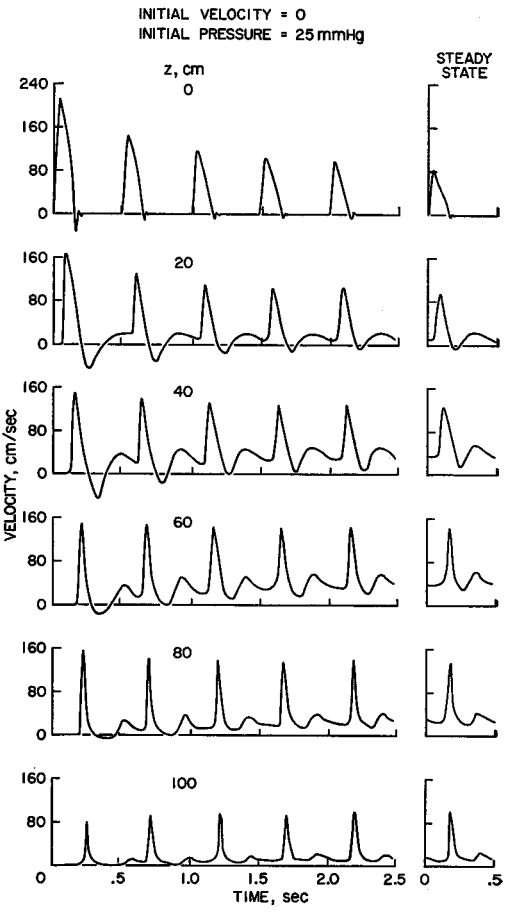

Figure 38
Velocity profiles for the Standard Case caused by a normal cardiac ejection pattern after a period of cardiac arrest sufficiently long to produce a quiescent state.

Case, we have computed the pressure and flow patterns over several heart beats. Figures 37 and 38 show the gradual return of the pressure and flow to steady state profiles. The approach to steady state appears to be roughly exponential. After five heart beats, the transient response still is approximately 5 mm Hg lower in pressure and about 5 cm/sec lower in velocity than the steady state values. However, life-sustaining pressures are evidently already attained after two or three heart beats.

There are significant differences between the shapes of the profiles during the first cardiac ejection and those occurring later. Most striking is the large velocity pulse in the vicinity of the heart, which can only be explained in terms of the narrowing of the aortic cross section at lower pressures. We also notice intervals of relatively large negative flows during the first few beats. In addition, the dicrotic wave occurs later relative to the primary pulse during the first few beats in this numerical experiment. By interpreting the dicrotic wave as a manifestation of some reflection phenomena, this delay may be attributable to the lower wave speeds of the reflected wave associated with the lower pressures in the beginning.

IX. Aortic Insufficiency and Shock Waves

It has already been noted that the system of one-dimensional differential equations for blood flow is hyperbolic, just as is the system of equations for the supersonic flow of a compressible fluid. Since the occurrence of shock waves is a familiar feature in high-speed compressible flow, it is reasonable to ask under what conditions similar phenomena could occur in the cardiovascular system. We know that in reality no true discontinuities can exist, but we can envision shock waves in the form of abrupt rises in pressure and flow or as spiketype perturbations which may evolve from relatively gradual changes in pressure.

While we have observed the steepening of the pressure wave for the Standard Case with increasing distance from the aortic valve, under normal conditions the pressure pulse generated by the heart is neither sufficiently steep nor strong to produce a shock wave within the dimensions of the body. However, in the case of an incompetent aortic valve (aortic insufficiency), the situation is quite different. The large amount of backflow associated with a leaking valve would reduce the normal net cardiac output per beat unless the size of the heart and the gross ejection volume are increased. A larger heart and correspondingly larger positive and negative flow rates are indeed clinically observed in patients with aortic insufficiency. Finally, any increase in the ejection volume for a given systolic time interval produces pressure pulses which are steeper and stronger than normal and can therefore generate shock waves within a shorter distance from the heart.

Lacking actual recordings of cardiac ejection patterns in instances of aortic valve incompetence, we have assumed the ejection rate function shown in Figure 39. We arrived at this function by utilizing the information given in Ref. [36], according to which regurgitation can exceed 80% of the net aortic flow. Also, the diastolic pressure at the heart should be of the order of 40 mm Hg or less to allow for the filling of the ventricle with oxygenated blood from the lung. In addition, we have kept the shape of the ejection curve approximately the same as in the Standard Case for the positive ejection phase of the cardiac cycle, but we increased the net stroke volume from 30 to 37.5 cm^3. All other cardiovascular parameters are identical with those of the Standard Case.

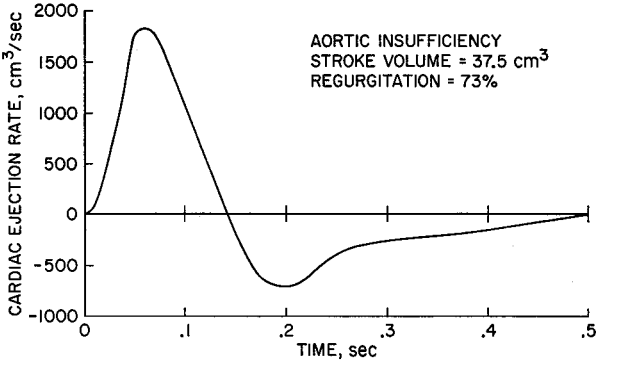

Figure 39
Hypothetical cardiac ejection rate pattern simulating aortic insufficiency. Amount of regurgitation is 73% of the gross stroke volume. Heart Rate 120 beats/minute.

Since the peak ejection rate is much higher, we expect a marked increase in pulse pressure as well as a much steeper wave front at the heart. Also, the inordinate regurgitation through the incompetent valve should cause significant backflow over a large segment of the aorta. These predictions are verified by the computed results, shown in Figures 40 and 41 together with the Standard Case. While normally the pressure remains elevated behind shock waves encountered in supersonic flow problems, it decays rapidly in our case due to the outflow and to the reversal in slope of the cardiac ejection curve.

For many years, it has been observed clinically that the so-called pistol shot phenomenon is associated with aortic valve incompetence. This phenomenon manifests itself with a sharp pulse which can actually deflect the palpating fingers at the radial or femoral artery. We can readily demonstrate that the pistol shot sounds must be generated locally. They cannot emanate from the heart, because they would be dissipated long before they could reach the extremities by the damping mechanism provided by the viscoelasticity of the arterial wall. The origin of the term 'pistol shot' stems from the sharp cracking sound heard through a stethoscope placed at the site. Just as an ordinary shock wave induces audible vibrations in air, the large and rapid rise in pulse pressure noted in Figure 40 can be expected to induce vibrations in the elastic arterial wall. When these vibrations are within the audible frequency range and have a sufficiently large amplitude, they represent a sound. Since the pressure pulse has a very peaked and narrow shape and is traveling at a speed of 5 to 15 meters per second, such a sound should be of very short duration. The findings here are in apparent agreement with clinical observations on the characteristics of the pistol shot

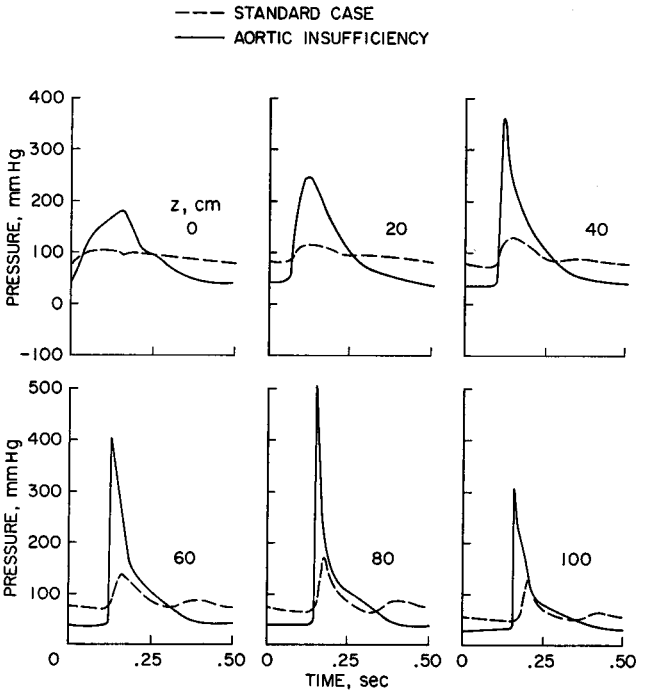

Figure 40
Pressure profiles for hypothetical aortic insufficiency corresponding to cardiac ejection rate given in Figure 39. Other parameter values are those for the Standard Case. First indication of a shock wave is suggested by the steepness of the pressure front at 40 cm from the heart.

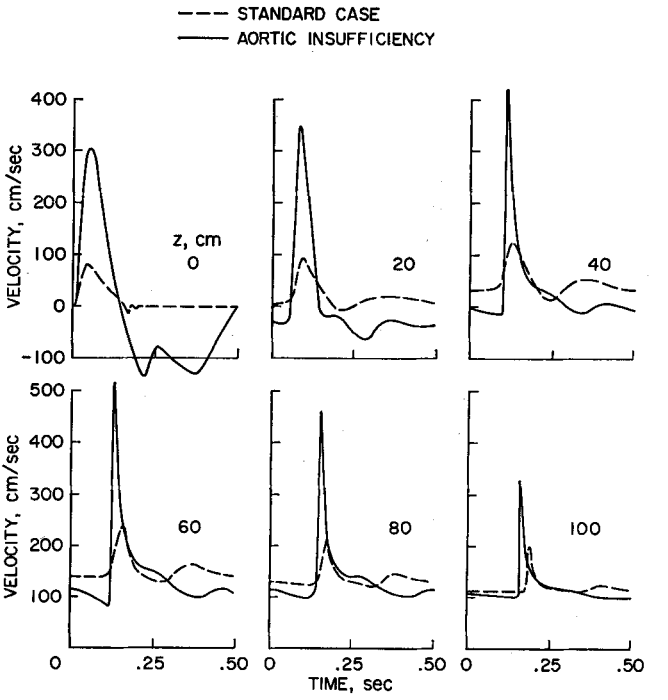

Figure 41
Velocity profiles for hypothetical aortic insufficiency corresponding to the pressure profiles of Figure 40. The flow pattern for $z = 0$ does not faithfully reproduce the ejection pattern imposed on the system and given in Figure 39. The apparent discrepancy however vanishes when we multiply the instantaneous flow velocity by the corresponding cross-sectional area. Our model allows for the variation of the cross-sectional area at the root of the aorta with pressure.

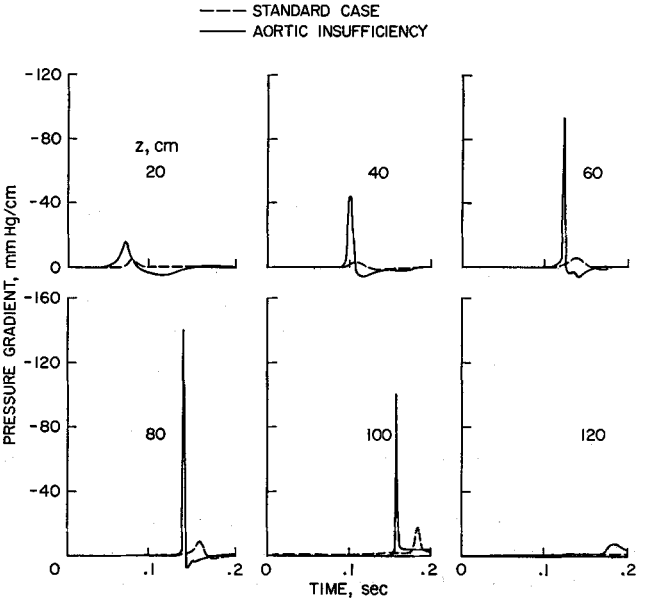

Figure 42
Local pressure gradients in the case of hypothetical aortic insufficiency.

sounds. Although we have been discussing the arterial pistol shot, a similar occurrence can arise on the venous side of the heart if the tricuspid valve is incompetent [22]. The venous pistol shot is normally detected over the jugular and femoral veins.

The development of the shock wave from a different viewpoint is shown in Figure 42 where we have plotted the local pressure gradient as a function of time on an expanded scale. (The local time rate of change of pressure $\partial p/\partial t$ would show similar features.) The differences from the Standard Case are very evident. For $z = 100$ and 120 cm, the gradient $\partial p/\partial z$ does not return immediately to zero because the pressure here is decreasing with distance. The difference in the travel times for the shock wave and the pressure pulse of the Standard Case is particularly noticeable in Figure 42. It is caused in part by the nonlinear effects of the variation of signal speed with pressure and velocity.

We can estimate the 'thickness' of the shock wave by multiplying the speed at which the wave travels relative to the fluid by the time necessary for its passage. The former can be approximated by the wave speed at the average pressure of the pulse, and the latter by the time interval during which the local pressure gradient exceeds 10% of its maximum value. Table 3 shows the results for this calculation. In com-

Table 3

Thickness of the arterial shock wave

Distance cm	Wave speed cm/sec	Time to pass sec	Thickness cm
0	340	.120	41
20	560	.025	14
40	900	.010	9
60	1100	.006	7
80	1700	.004	7
100	1200	.005	6
120	670	.030	20

pressible flow problems, the shock wave thicknesses are extremely small compared to the physical dimensions of the bodies involved. The thicknesses given in Table 3 are much larger, of the order of ten times the arterial diameter. They also indicate that the shock wave does not form abruptly, but in a gradual manner. In the case considered, it approaches a minimal thickness of about 6 cm and then broadens again.

The peak pressures exceed 500 mm Hg at $z = 80$ cm and as such are probably somewhat high. Presumably this may partly be due to the fact that we have disregarded the viscoelastic damping in the wall, which is particularly pronounced for spike-type perturbations. Yet, it should be mentioned that systolic pressures beyond 300 mm Hg have been observed in man [37]. In general, the gross features associated with aortic insufficiency predicted here for the dog seem to be in qualitative agreement with observations on man. Even the fact that backflow is still present for $z = 60$ cm (near the external iliac artery) appears to be realistic [37].

X. Discussion and Conclusions

The results of this study have shown that the familiar features of the natural pressure and flow pulses in arteries can be reproduced mathematically with the help of the method of characteristics if we specify the physical and geometric cardiovascular parameters properly. In examining the effects of changes in these parameters, it became apparent that the incisura develops even when there is no backflow as long as the time interval of diminishing ejection rate is sufficiently short. This means that towards the end of cardiac ejection, the flow rate (Figure 7) must decay rapidly to zero to give rise to an incisura. Also, for the wave speeds considered, we did not observe the phenomenon of backflow in the aorta beyond a distance of 30 cm from the heart except at low heart rates, low pressures, and in the presence of incompetent aortic valves. Generally speaking, for stiffer arteries the backflow was less pronounced and vanished at shorter distances from the heart.

When we take the nonlinear effects into account, we can always notice a marked steepening of the wave front and a peaking of the pulses as they propagate. By contrast, the linearized analysis predicts less peaking of the pulse and essentially no steepening of the wave front. It also yields a significantly different diastolic pressure, a wider pulse, and a more prominent dicrotic wave. These differences between the results of a linear and a nonlinear treatment of the propagation of large-amplitude pressure waves suggest that nonlinear effects must be accurately accounted for if we are interested in the interpretation of small changes in the flow and pressure pulses.

Many of the features of the dicrotic wave indicate that it is caused by the reflection of the primary pressure pulse from the more distal regions of the arterial tree. However, the quantitative aspects of this reflection phenomenon are not yet established and additional investigations will be necessary. As we do not observe a dicrotic wave when the model artery is infinitely long and has neither taper nor outflow, we may infer that the dicrotic wave is a consequence of taper or outflow. Also, since the dicrotic wave appears progressively later in time with increasing distance from the heart, it cannot be the result of a discrete reflection from a single site. This conclusion is also supported by the fact that the dicrotic wave occurs essentially at the same time for a given distance from the heart, irrespective of whether we impose the terminal boundary condition at 71, 103, 120 or 150 cm from the heart.

It is questionable whether the effects of fluid viscosity have been accounted for in a satisfactory manner since the friction expression is based on the assumption of quasi-steady flow. For a nominal value of $\mu = .049$ poise or less, the results are essentially the same for laminar or turbulent flow. However, when we increase the effective viscosity coefficient to 0.49 poise, then the pulse waves exhibit a much more rapid decay with distance for laminar flow than in the turbulent case; yet, the basic shape of the pressure and flow pulses is not markedly altered.

The concept of a peripheral resistance for the distal boundary condition was found to be remarkably satisfactory provided that this boundary condition was applied no closer to the heart than the femoral region in the cases examined. Attempts to utilize a peripheral resistance in the abdominal aorta yielded drastic alterations in the pressure and flow patterns.

The wave front velocity for the Standard Case compared rather favorably with experimentally obtained data. Likewise, harmonic analyses of the computed results for various stations along the artery show that the apparent phase velocities of the different harmonics as well as the impedances resemble those obtained from dog experiments.

A decrease of 36% in cross-sectional area of the artery and an increase in arterial wall stiffness corresponding to a 40% rise in wave speed produced substantial changes in the pressure and flow pulses, suggesting that they may possibly serve as diagnostic indicators. The potential use of the flow pulse for diagnostic purposes seems particularly promising in view of the recent development of ultrasound echo-ranging devices [5] and pulsed doppler flowmeters [3]. Both the reduction in diameter and the increase in wave speed effectively produced a diminished distensibility causing an elevation of the pulse pressure in the major arteries as predicted by the model. Whereas the increase in wave speed primarily affected the shape of the flow pulse and only slightly the peak flow velocities, the reduction in diameter mainly increased the peak flow velocities and left the shape of the flow pulse essentially unchanged. Figures 23 and 24 hint that a sufficiently large increase in wave speed might lead to the development of a second dicrotic wave. They also demonstrate that backflow can virtually be eliminated by raising the wave speed. Moreover, they clearly show that relatively small changes in the pressure gradient alter extensively the flow pattern. This again suggests that the results to be obtained by prescribing the pressure variation at the root of the aorta (instead of specifying the ejection pattern) as a boundary condition may exhibit large errors in the predicted flow pattern unless we know the pressure at the heart with extreme accuracy. In addition, it shows that the pressure gradient technique for determining the cardiac output [38] is prone to large errors.

The simulation of rest and of exercise by considering pulse rates of 60 and 180 beats per minute and modifying the resistance of the vascular bed to enforce normal pressure levels revealed distinct changes in the pressure and flow pulses. The lower heart rate produced significantly higher pulse pressures and larger dicrotic waves but much smaller average flow velocities as compared with the Standard Case. It also allowed for backflow at distances beyond 40 cm from the heart. In addition, as sometimes observed experimentally [27], multiple diastolic (dicrotic) waves, which may even exhibit backflow, are predicted at the lower heart rate. The higher pulse rate simulating exercise produced generally opposite effects, i.e., lower pulse pressures, higher mean flow velocities, reduced backflow, and a smaller dicrotic wave.

Overall modifications of the outflow resistance as might be caused by vasoconstriction, vasodilatation, and by removing an abdominal organ seem to yield the expected changes in the pressure level but only mild alterations in the flow patterns.

Cardiac arrest and the subsequent resumption of the normal heart beat were simulated to seek evidence of transient phenomena. When the heart is stopped, extra waves which are normally obscured by following heart beats are observed, but they have very small amplitudes. This suggests that they are caused by multiple reflections of the primary pressure pulse and that the dicrotic wave is the first of these reflections. When the normal cardiac ejection is resumed after a quiescent state of uniform pressure of 25 mm Hg and zero velocity has been reached, it takes only 2 or 3 heart beats to restore the pressure and flow pulses to life-sustaining levels.

Simulating aortic insufficiency, we find that the wave front is rapidly steepened with increasing distance from the heart in a fashion reminiscent of shock waves in high-speed compressible flow. Indeed, a first indication of a shock wave in our particular case could be observed at 40 cm from the heart. Its effective thickness was estimated to be as small as 6 cm. The occurrence of shock waves in our model of the cardiovascular system should not be too surprising since the governing differential equations form a hyperbolic system. Normally, the dimensions of the body are too small to allow for the development of a shock wave. It is only in cases of circulatory disorders such as aortic insufficiency, where we have a very steep pressure front at the heart and an unusually large pulse pressure, that a shock wave can develop within a realistic distance from the heart.

Acknowledgements

This work was carried out at the Ames Research Center of NASA with the support of NASA Grant NGL 05-020-223.

The authors are indebted to Dr. H. N. Hultgren, Cardiology Division, Stanford University School of Medicine, for his comments and suggestions. They also wish to thank Miss M. Kathleen Hunt for her help in typing and editing the manuscript.

Some excerpts from this paper have been presented at the AGARD Specialists' Meeting on Fluid Dynamics of Blood Circulation and Respiratory Flow in Naples, Italy, 4–6 May 1970.

References

The complete list is published with Part I, Z. ang. Math. Phys. *22*, 245 (1971),

Zusammenfassung

In jeder Gruppe von Menschen variieren die Kreislaufparameterwerte von Individuum zu Individuum ziemlich stark. Um die Effekte realistischer Schwankungen dieser Parameter auf die Strom- und Druckpulse in arteriellen Leitungen zu untersuchen und um mögliche Manifestationen gewisser pathologischer Zustände wie Arteriosklerosis und die Insuffizienz der Aortenklappen zu identifizieren, werden hier einige der Resultate präsentiert, die sich auf Grund des im ersten Teil beschriebenen mathematischen Modells ergeben. Insuffizienz der Aortenklappen ist nachgebildet durch einen Ausströmungspuls mit aussergewöhnlich grossem Rückstrom. Der zugehörige Druckpuls zeigt die bekannten Eigenschaften von Stosswellen, die anscheinend verantwortlich sind für die «pistol shot sounds», die man über der arteria femoralis und der arteria radialis von Patienten mit Aorteninsuffizienz hört.

(Received: June 8, 1970)